17th Australasian Fluid Mechanics Conference
Auckland, New Zealand
5-9 December 2010

A Three-Dimensional Transient Growth and DNS Analysis of 'High Tail' and 'Flat Tail' Aircraft Configurations

Chris L. Ellis, Kris Ryan and Gregory J. Sheard

Fluids Laboratory for Aerospace and Industrial Research, Department of Mechanical and Aerospace Engineering, Monash University, Clayton, Victoria, 3800, Australia

Abstract

This paper investigates the transient growth response of perturbations added to counter-rotating four vortex systems. The paper also compares the transient response of the wakes behind 'high tail' configuration aircraft, such as the C-17 Globemaster, with that of the wakes behind more conventional 'flat tail' aircraft, such as the Boeing 747-400. Transient growth is computed using the method of Barkley *et al.* [*Int. J. Numer. Meth. Fluids* **57**, 1435–1458], and this is the first application of this method to multiple vortex pair systems.

The study conducted found that when the perturbations found from the transient growth analysis that lead to optimal energy growth are used to perturb a four vortex system then the perturbations grow rapidly and have a significant effect on the base vortex system. It also found that when the vortex pair that simulates the vortices shed off an aircraft tail is vertically displaced, the growthrate of the perturbations is approximately double that of the 'flat tail' configuration in a three-dimensional direct numerical simulation.

Introduction

Wake vortices are a byproduct of the generation of lift by the wings of an aircraft. They are produced when the high pressure air from underneath the wing flows around the outer edges of the wing tip. This causes a coherent vortex structure that extends almost horizontally behind the aircraft to form and can linger in the air for some time far downstream of the aircraft path [12]. The circulations generated by these vortices can pose a real danger to following aircraft, as evidenced by the crash of an American Airlines Airbus A300 in New York, on 12 November 2001, due to a structural failure of its rudder when abrupt corrections were applied after passing through another aircraft's wake (NTSB Report Number AAR-04-04). As aircraft are becoming larger and larger, the wake vortices they produce are also increasing in size and strength. This limits the maximum passenger throughput of airports, and therefore motivates research into mechanisms for reducing the impact of these vortices in aviation. Counter-rotating vortex pairs, as a model for aircraft wakes, have been investigated since the 1970s [1]. More recently, it has been shown that the strength of the vortex pair produced from the tail of an aircraft can be anywhere up to 50% of the strength of the vortex pair produced by the wings [13]. The presence of the vortex pair extending from the tail can have a significant effect on the two dimensional kinematic properties of the stronger vortex pair shed by the wings. While this has been investigated by Fabre *et al.* [6], and Crouch [4], the focus has been on potential ways to force three-dimensional instabilities to form in the main wing vortex pair. To date, no research has investigated how a change in the aircraft tail configuration affects the overall vortex system.

For aircraft such as the C-17 Globemaster heavy lift aircraft, the tail can offset vertically from the plane of the wings by up to 20% of the span of the wings. This research is particularly pertinent to military airfields where the majority of the aircraft are either very large high tail heavy lift aircraft such as the C-17, or much smaller fighter type aircraft. An understanding of the stability of these flows is of interest as it can provide insight into possible mechanisms for the disruption of these types of flows to reduce the hazard for trailing aircraft.

Crouch [4] employed a vortex filament model to study the stability and transient growth of a system comprising two co-rotating vortex pairs. This type of four-vortex system is representative of the vortex system generated by an aircraft from the wingtips and any discontinuity along the wing surface, such as flaps. The vortex filament model is limited as it does not go down to the scale within the vortex core and is limited to sinuous instability modes. Crouch used a Floquet type analysis to look at the stability of the vortex system. A limitation of this analysis is that it assumes a time-periodic flow. However, vortex wakes are subject to diffusion from the moment they form and thus strictly lack the time periodicity required for a Floquet-type linear stability analysis.

Given the gradual erosion of the vortex system by diffusion, and the interest in mechanisms for the rapid destruction of these vortex systems, a transient growth analysis is well suited to the study of this type of flow. Transient disturbances in these types of flow can be very important as they have the potential to severely alter the baseflow and cause destruction of the wake vorticies. Barkley *et al.* [2] proposed a method of transient growth analysis that is based on an eigenvalue solution of a time-integrated disturbance field, which is readily implemented using a straightforward modification of a standard Floquet analysis solver. This technique has been further applied to the study of steady and pulsatile stenotic flows [5] and flow over a backward-facing step [3]. This method has not yet been applied to vortex systems, particularly the four-vortex system investigated here.

Methodology

The vortex system comprises two pairs of counter-rotating vortices with circulation magnitude Γ_1 and Γ_2. Figure 1 shows a schematic representation of the vortex system under investigation and the key variables defining the problem. The system is evolved using the incompressible Navier-Stokes equations.

$$\frac{\partial \mathbf{u}}{\partial t} = -(\mathbf{u}\cdot\nabla)\mathbf{u} - \nabla p + \upsilon\nabla^2\mathbf{u}, \quad (1)$$

$$\nabla\cdot\mathbf{u} = 0, \quad (2)$$

where $\mathbf{u}$ is the velocity vector field, t is time, p is the kinematic pressure and υ is the kinematic viscosity.

A Gaussian vortex profile was used, which was chosen to be consistent with previous work in the area [6, 8, 19]. Moreover, LeDizès & Verga [12] demonstrated that arbitrary vortex profiles attract to a Gaussian profile, making it a generic representation of a vortex. The other advantage with this type of vortex profile is

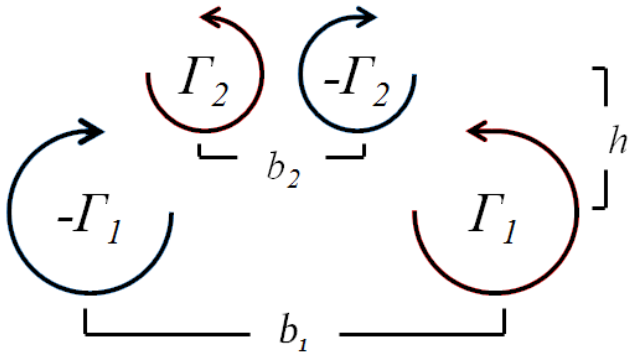

Figure 1: Schematic diagram of the four-vortex system considered in this study. Symbols are used to define vortex circulations and spacings are shown.

that it allows for the analysis of all of the Kelvin mode instabilities, not just sinuous modes. The tangential velocity around a Gaussian vortex is given by

$$v = \frac{\Gamma}{2\pi r}\left(1 - e^{\left[-\left(\frac{r}{r_0}\right)\right]^2}\right), \qquad (3)$$

where v represents the tangential velocity, r is the radius from the centre of the vortex and r_0 is the vortex core size.

In this study, *Re* is defined based on the circulation magnitude of the larger vortex pair Γ_1, and the kinematic viscosity, υ, as,

$$Re = \frac{\Gamma_1}{\upsilon}. \qquad (4)$$

A Reynolds number, Re = 20,000, was employed in this study, consistent with the ranges used in previous studies on counter-rotating vortices [16, 13, 9]. This value allowed for reasonable computational resources and computation time. It is assumed that the instabilities being investigated are consistent across the *Re* of a real aircraft and the simulations. This assumption is reasonable as the primary method of destruction of this type of vortex system is caused by perturbations with wavelengths that are far above the turbulence length scales damped out by the higher viscosity [11].

The problem is simulated using an in-house code employing a spectral-element discretization in space and a third-order time-integration scheme based on backward differentiation. This type of solver has been used extensively to study myriad wake and vortex flows [17, 18, 19]. The solver employs a nodal formulation, in which Lagrangian tensor-product polynomials are employed in each element. The degree of this polynomial can be changed for a given simulation to control spatial resolution. More information on this method can be found in Karniadakis *et al.* [10].

The method utilised to find the perturbation fields that lead to optimum transient growth of an integral norm of energy was described in Barkley *et al.* [2]. Global linear stability analysis predicts the asymptotic stability of a flow, which is goverened by only the leading eigenmode of the linear evolution operator. However, large amplitude transient growth is possible over short times due to the interaction between the non-normal eignemodes of the system, and it is this short-timescale amplification that is the focus of this study. The eigenvalue solver used in this study has been validated and employed in the past in linear stability analysis of other flows [17], and has produced results consistent with an independent formulation of the algorithm [4].

This method begins by defining an operator $\mathcal{A}$(t) describing the evolution of a perturbation field,

$$u'(t) = \mathcal{A}(t)u'(0). \qquad (5)$$

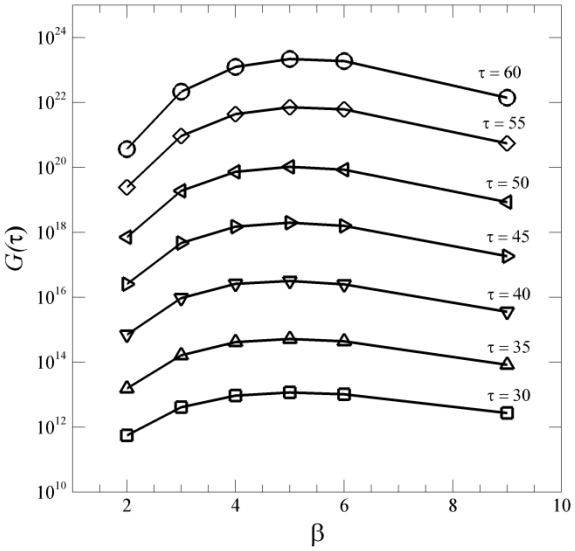

Figure 2: Plot of `flat tail' transient growth amplification factor, $G(\tau)$, against wavenumber, β, for the indicated time intervals.

The norm used by Barkley *et al.* [2] to quantify the size of a perturbation is the total kinetic energy of the perturbation field.

By normalizing the energy growth of the perturbation with its initial energy and using the evolution operator such that,

$$\frac{E(\tau)}{E(0)} = \left(\mathcal{A}(\tau)u'(0), \mathcal{A}(\tau)u'(0)\right) = \left(u'(0), \mathcal{A}^*(\tau)\mathcal{A}(\tau)u'(0)\right), \qquad (6)$$

(where $\mathcal{A}^*(\tau)$ is the adjoint evolution operator to $\mathcal{A}(\tau)$ in the L^2 norm) it becomes possible to find the dominant eigenvalues of $\mathcal{A}^*(\tau)$ $\mathcal{A}(\tau)$ which dictate the largest possible transient growth for a perturbation at given τ value.

The action of the evolution operator, $\mathcal{A}$(t), on the perturbation vector is equivalent to integrating the linearized Navier--Stokes equation forward in time. Given this, the effect of the adjoint to this operator, $\mathcal{A}^*$(t), on the perturbation vector is the equivalent of integrating the adjoint Navier-Stokes equation backwards in time over the time, τ. Due to the requirement to integrate backwards in time, interpolation is used to supply the base flow velocity field for the adjoint operation. Ultimately, this method uses the same principles as linear stability analysis, except the eigenmodes that are being computed are that of $\mathcal{A}^*(\tau)$ $\mathcal{A}(\tau)$, rather than that of $\mathcal{A}(\tau)$.

Results

It can be seen in Figure 2 that as τ increases, the general trend of the growth amplification factor against wavenumber remains the same, giving a log-linear increase in the growth amplification factor with increase in τ. Another point of note is that the peak wavenumber is independent of τ.

From the perspective of flow control, this implies that a system need only perturb at a frequency corresponding to a specific axial wavenumber to effectively disrupt the baseflow. For a `flat tail' case, the wavenumber is approximately 5. It is important to note that the peak growth amplification factor for higher τ values is of sufficient magnitude as to cause significant changes to the baseflow, causing rapid destruction of the wake vortex system. This large growth however will violate the linear model of the disturbance and a full three-dimensional simulation is required to determine the actual energy amplifications resulting from these disturbances. These three-dimensional simulations are covered later in this paper.

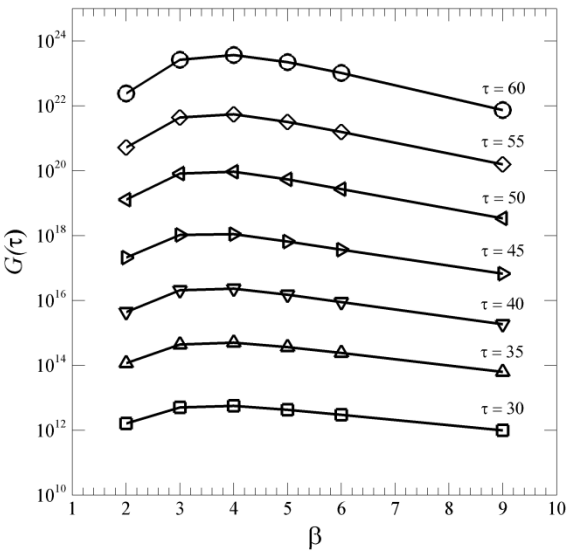

Figure 3: Plot of 'high tail' transient growth amplification factor, $G(\tau)$, against wavenumber, β, for the indicated time intervals.

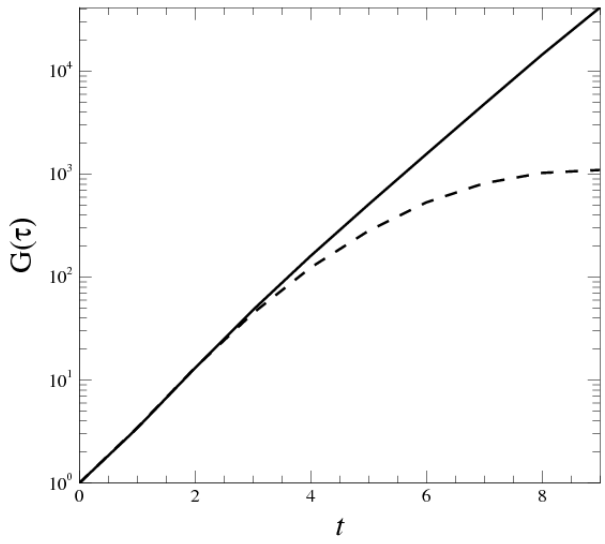

Figure 4: Plot of `flat tail' perturbation energy normalized by initial energy. The solid line represents the solution of the linearized Navier-Stokes equation and the dashed line represents the energy in the Fourier modes of the three dimensional direct numerical simulation. The solution of the linearized Navier-Stokes equation was conducted at $\tau = 60$ and at $\beta = 5$.

It can be seen in Figure 3 that the 'high tail' transient growth amplification factor shows similar qualitative trends to the 'flat tail' case. It does however have important quantitative differences, such as the peak wavenumber being closer to 3.5. This indicates that an active control method to induce destruction of an aircraft wake would need to be tailored to the aircraft tail configuration. It is interesting to note that the peak $G(\tau)$ of the `high tail' is less than that of the `flat tail' for a τ of less than 55, while peak $G(\tau)$ is higher in the `high tail' case for a τ of greater than 55. This indicates that for an initial perturbation added to the system, the `high tail' case will have greater energy growth, potentially leading to a shorter-timescale for the destruction of the vortices.

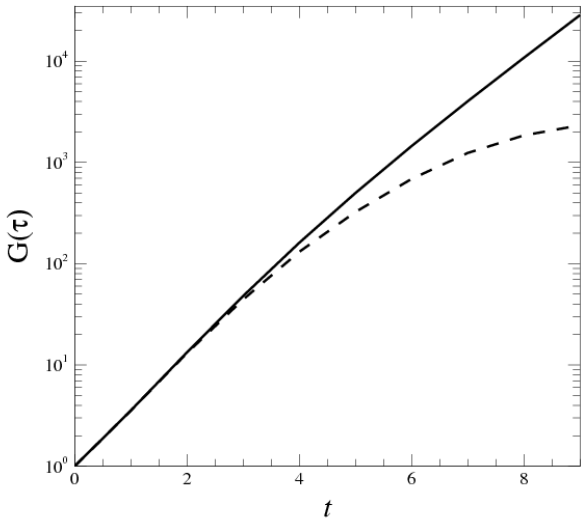

Figure 5: Plot of `high tail' perturbation energy normalized by initial energy. The solid line represents the solution of the linearized Navier-Stokes equation and the dashed line represents the energy in the fourier modes of the non-linear simulation. The solution of the linearized Navier-Stokes equation was conducted at $\tau = 60$ and at $\beta = 3.5$.

Figures 4 and 5 show the energy in the perturbations, normalized by the initial energy, compared to the energy in the non-zero Fourier modes of the three dimensional direct numerical simulation for the `flat tail' and `high tail' cases respectively. The perturbation fields become highly non-linear after less than 25% of the time it takes for the tail vortex pair to orbit the wing vortex pair, with the `high tail' case having more energy, leading to faster instability growth and destruction of the vortex system. It is interesting to note that the optimal perturbation fields found from the linearized Navier-Stokes equations continue to grow even though the baseflow becomes changed. This means that the perturbation initialised by the optimal perturbation fields found with the linearized Navier-Stokes equations continues to grow even with the large changes to the baseflow until the flow structures become small enough for the fluid viscosity to damp out. It is possible for the perturbations to change the baseflow in such a way that would not be conducive to growth and the energy in the perturbations would slowly decay due to the fluid viscosity.

It is interesting to note that the energy in the 'high tail' configuration is approximately double that of the 'flat tail' configuration. This implies that an optimal disturbance in the wake from a 'high tail' aircraft will cause the destruction of the vortex structure in a shorter period of time, leading to faster viscous dissipation.

Figure 6 shows the 'flat tail' configuration at times $t = 0$ and 7. As can be seen, even after such a short timeframe, the flow becomes highly turbulent when a small initial optimal perturbation is added. The high level of small turbulence structure after 7 time units allows the viscosity of the fluid to assist in the destruction of the flow.

Figure 7 shows the 'high tail' configuration at times $t = 0$ and 7. As can be seen, even after such a short timeframe, the flow becomes highly turbulent when a small initial optimal perturbation is added.

It is also important to note that the bulge in the larger vortex pair compared to the 'flat tail' case indicates that the transient growth is having a larger effect on the 'high tail' case. This suggests that the 'high tail' case is more susceptible to transient growth and therefore will be destroyed in a shorter timeframe.

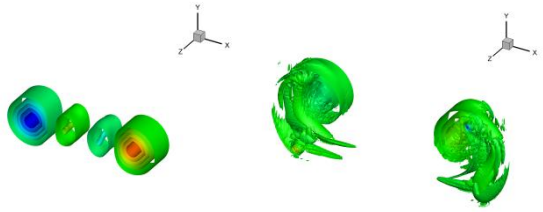

Figure 6: Flooded contour Plot of isosurfaces of axial vorticity of the 'flat tail' three-dimensional DNS. The left plot is at $t = 0$, the right plot is at $t = 7$. Contour levels were arbitrarily chosen to best display the flow structures. Red represents positive (anti-clockwise) vorticity and blue represents negative (clockwise) vorticity.

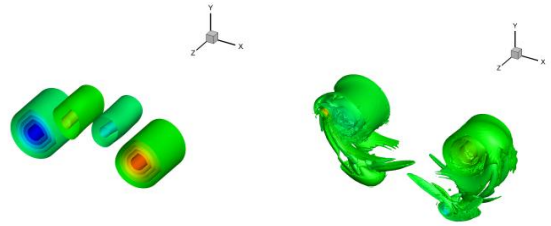

Figure 7: Flooded contour Plot of isosurfaces of axial vorticity of the 'high tail' three-dimensional DNS. The left plot is at $t = 0$, the right plot is at $t = 7$. Contour levels were arbitrarily chosen to best display the flow structures. Red represents positive (anti-clockwise) vorticity and blue represents negative (clockwise) vorticity.

Conclusions

This paper investigated the non-linear response of four vortex systems to the perturbations that lead to optimal energy growth predicted using a transient growth analysis.

While the transient growth analysis is conducted using the linearised Navier-Stokes equations, the perturbations that lead to optimal energy growth continue to gain energy even though the baseflow becomes massively perturbed. This is an interesting discovery as the changes in the baseflow could have produced an environment that is not conducive to the growth of the perturbation, damping it out and having little further effect on the baseflow.

The data shows that the energy in the perturbations for a 'high tail' wake grows at a slightly faster rate than the 'flat tail' configuration. This implies that the transient growth of the perturbation will cause the vortex structure to break down into smaller turbulent structures in a shorter time, allowing viscous dissipation to reduce the hazard to trailing aircraft.

Acknowledgement

The authors would like to acknowledge the Monash University E-research centre for the access to its high performance computing cluster, Sungrid and the MeRC High Performance Computing Scholarships to conduct this research. Also the authors would like to thank the Monash University faculty of engineering for the Faculty of Engineering Small Grant.

References

[1] Barker, S.J. and Crow, S.C., 1977, The motion of two-dimensional vortex pairs in a ground effect, Journal of Fluid Mechanics, *J. Fluid Mech.*, **82**, 659-671

[2] Barkley, D., Blackburn, H.M. & Sherwin, S.J. 2008, Direct optimal growth analysis for timesteppers. *Int. J. Numer. Meth. Fluids* **57**, 1435–1458.

[3] Blackburn, H.M., Barkley, D. & Sherwin, S.J. 2008*a* Convective instability and transient growth in flow over a backward facing step. *J. Fluid Mech.* **603**, 271–304.

[4] Blackburn, H.M. & Sheard, G.J. 2010 On quasi-periodic and subharmonic floquet wake instabilities. *Phys. Fluids* **22(3)** (031701:1-4).

[5] Blackburn, H.M., Sherwin, S.J. & Barkley, D. 2008*b* *C*onvective instability and transient growth in steady and pulsatile stenotic flows. *J. Fluid Mech.* **607**, 267–277.

[6] Crouch, J.D. 1997 Instability and transient growth for two trailing-vortex pairs. *J. Fluid Mech.* **350**, 311–330.

[7] Donnadieu, C., Ortiz, S., Chomaz, J., & Billant, P., 2009, Three dimensional instabilities and transient growth of a counter-rotating vortex pair. *Phys. Fluids* **21** (094102).

[8] Fabre, D., Jaquin, L. and Loof, A., 2002, Optimal perturbations in a four-vortex aircraft wake in counter-rotating configuration, *J. Fluid Mech.*, **451**, 391-328.

[9] Haverkamp, S., Neuworth, G. & Jacob, D. 2005, Active and passive vortex vortex wake mitigation using control surfaces. *Aerospace Science and Technology* **9**, 5–18.

[10] Karniadakis, G.E., Israeli, M. & Orszag, S.A. 1991, High-order splitting methods for the incompressible Navier-Stokes equations. *J. Comp. Phys.* **97**, 414–443.

[11] Landman, M.J. & Saffman, P.J. 1987, The three-dimensional instability of strained vortices in a viscous fluid. *Phys. Fluids* **30(8)** (082339)

[12] LeDizès, S. & Verga, A. 2002, Viscous interactions of two co-rotating vortices before merging. *J. Fluid Mech.* **467**, 389–410.

[13] Lele, S.K., 2001, Vortex-wake pollution: A problem in fluid mechanics. *Lecture Notes in Physics -New York then Berlin-* pp. 163–182.

[14] McCormick, B.W. 1995 *Aerodynamics, Aeronautics and Flight Mechanics*, 2nd edn. John Wiley & sons, Inc.

[15] Rennich, S.C. & Lele, S.K. 1999 A method for accelerating the destruction of aircraft wake vortices. *J. Aircraft* **36**, 398–404.

[16] Roy, C., Schaeffer, N., Le Dizès, S. & Thompson, M. 2008, Stability of a pair of co-rotating vortices with axial flow. *Phys. Fluids* **20** (094101).

[17] Sheard, G.J., Fitzgerald, M.J. & Ryan, K. 2009 Cylinders with square cross section: Wake instabilities with incidence angle variation. *J. Fluid Mech.* **630**, 43–69.

[18] Sheard, G.J., Leweke, T., Thompson, M.C. & Hourigan, K. 2007 Flow around an impulsively arrested circular cylinder. *Phys. Fluids* **19(8)** (083601).

[19] So, J., Ryan, K. & Sheard, G.J. 2008, Linear stability analysis of a counter rotating vortex pair of unequal strength. *ANZIAM J.* **50**, C137–C151.